THE JOURNAL OF BIOLOGICAL CHEMISTRY VOL. 286, NO. 33, pp. 28738–28748, August 19, 2011

Activity-dependent Phosphorylation of Neuronal Kv2.1 Potassium Channels by CDK5*

Received for publication, April 15, 2011, and in revised form, June 22, 2011 Published, JBC Papers in Press, June 28, 2011, DOI 10.1074/jbc.M111.251942

Oscar Cerda[‡] **and James S. Trimmer**[‡§1]

From the Departments of [‡]*Neurobiology, Physiology, and Behavior, and* [§]*Physiology and Membrane Biology, University of California, Davis, California 95616*

Dynamic modulation of ion channel expression, localization, and/or function drives plasticity in intrinsic neuronal excitability. Voltage-gated Kv2.1 potassium channels are constitutively maintained in a highly phosphorylated state in neurons. Increased neuronal activity triggers rapid calcineurin-dependent dephosphorylation, loss of channel clustering, and hyperpolarizing shifts in voltage-dependent activation that homeostatically suppress neuronal excitability. These changes are reversible, such that rephosphorylation occurs after removal of excitatory stimuli. Here, we show that cyclin-dependent kinase 5 (CDK5), a Pro-directed Ser/Thr protein kinase, directly phosphorylates Kv2.1, and determines the constitutive level of Kv2.1 phosphorylation, the rapid increase in Kv2.1 phosphorylation upon acute blockade of neuronal activity, and the recovery of Kv2.1 phosphorylation after stimulus-induced dephosphorylation. We also demonstrate that although the phosphorylation state of Kv2.1 is also shaped by the activity of the PP1 protein phosphatase, the regulation of Kv2.1 phosphorylation by CDK5 is not mediated through the previously described regulation of PP1 activity by CDK5. Together, these studies support a novel role for CDK5 in regulating Kv2.1 channels through direct phosphorylation.

Plasticity in the intrinsic excitability of neurons comprises experience-dependent changes in how individual neurons integrate and process synaptic input and determine their mode of output, and involves dynamic changes in the expression, localization, and/or functional properties of voltage-gated ion channels. Kv2.1, a delayed rectifier-type voltage-gated potassium or Kv channel expressed in high density clusters in somatodendritic domains of mammalian neurons (1–3), is subjected to rapid activity-dependent, calcineurin-dependent dephosphorylation, resulting in a more hyperpolarized threshold for activation of Kv2.1 currents and loss of clustering (4–12) and leading to homeostatic suppression of neuronal firing (6, 13). Removal of these stimuli leads to recovery of Kv2.1 phosphorylation and clustering (5, 7, 9, 10, 12). Anesthesia *in vivo* induces enhanced Kv2.1 phosphorylation (7), showing that bidirectional changes in neuronal activity trigger homeostatic changes in the Kv2.1 phosphorylation state. Modulation of Kv2.1 is the candidate mechanism for plasticity in the intrinsic excitability of visual cortical neurons in response to monocular deprivation and in long term potentiation of intrinsic excitability (14).

Liquid chromatography-tandem mass spectrometry (LC-MS/MS)-based analyses have defined a large set of *in vivo* Ser and Thr Kv2.1 phosphorylation sites (15, 16), a subset of which are dephosphorylated upon calcineurin activation and mediate the activity-dependent changes in Kv2.1 localization and function (7, 15). Among these sites, phosphorylation at the Ser-603 residue exhibits extraordinary sensitivity to bidirectional activity-dependent changes in phosphorylation state (7). The protein phosphatases (PPs)[2] PP1 and calcineurin/PP2B have been identified as playing crucial and non-overlapping roles in constitutive and activity-dependent dephosphorylation of Kv2.1, respectively (5, 7). However, the specific protein kinases (PKs) responsible for constitutive and activity-dependent phosphorylation of Kv2.1 have not been identified.

Among the identified Kv2.1 phosphorylation sites, almost half (including Ser-603) are adjacent to a C-terminal Pro residue, suggesting phosphorylation by Pro-directed Ser/Thr PKs. Among these, cyclin-dependent kinase 5 (CDK5) is a neuronal PK whose activity depends on association with myristoyl-anchored p35 and p39 cofactors and whose activity underlies diverse aspects of neuronal biology, including neurogenesis, neuronal migration and survival, synaptic plasticity, and neurodegeneration (17–19). Here, we investigate the role of CDK5 in the constitutive and activity-dependent phosphorylation of Kv2.1 and define a new role for CDK5 in regulating neuronal function through direct phosphorylation of a voltage-gated ion channel crucial to activity-dependent plasticity in intrinsic neuronal excitability.

EXPERIMENTAL PROCEDURES

Materials—All materials were reagent grade and obtained from Sigma or Roche Applied Science except where noted. PK and PP inhibitors (roscovitine, FK520, and okadaic acid) were obtained from Calbiochem.

Cell Culture and Plasmids—HEK293 cells were grown at 37 °C and 5% CO_2 in DMEM high glucose medium (Invitrogen) supplemented with 10% fetal bovine serum and were transiently transfected with pRBG4/Kv2.1 (20), pcDNA-GFP-CDK5-D144N, pcDNA3-GFP-CDK5, pCMV-myc-p35, pcDNA-myc-PP1, and pcDNA-myc-PP1 (T320A) plasmids using Lipofectamine 2000 (Invitrogen) according the manufacturer's instructions.

* This work was supported, in whole or in part, by National Institutes of Health Grant NS42225 (to J. S. T.).

[1] To whom correspondence should be addressed: Dept. of Neurobiology, Physiology, and Behavior, 196 Briggs Hall, University of California, One Shields Ave., Davis, CA 95616-8519. E-mail: jtrimmer@ucdavis.edu.

[2] The abbreviations used are: PP, protein phosphatase; AP, alkaline phosphatase; PK, protein kinase; RBM, rat brain membrane; HBSS, Hanks' buffered saline solution; DIV, days *in vitro*; RSB, reducing SDS sample buffer; DPBS, Dulbecco's phosphate-buffered saline; TTX, tetrodotoxin.

Antibodies—For immunofluorescence labeling and immunoblot experiments, we used as primary antibodies rabbit anti-MAP2 (Millipore, Billerica, MA) and anti-Kv2.1 KC (21) polyclonal antibodies, mouse anti-Kv2.1 (K89/34), and anti-GRP75 (N52A/42) mAbs (University of California Davis/National Institutes of Health NeuroMab Facility, Davis, CA), mouse anti-Kv2.1 K89/41 mAb, and rabbit phosphospecific pS603 polyclonal antibody (7, 15). Alexa-conjugated secondary antibodies (Invitrogen) were used for immunofluorescence staining, and horseradish peroxidase-conjugated secondary antibodies (KPL, Gaithersburg, MD) were used for immunoblotting.

Neuronal Culture—All animal use procedures were in strict accordance with the National Institutes of Health Guide for the Care and Use of Laboratory Animals and were approved by the Institutional Animal Care and Use Committee of the University of California Davis. Hippocampi were dissected from embryonic day 18 rat embryos and dissociated enzymatically for 15 min at 37 °C in 0.25% (w/v) trypsin (Invitrogen) in Ca^{2+}/Mg^{2+}-free HBSS and mechanically by triturating with Pasteur pipettes. The dissociated cells were washed twice in Ca^{2+}/Mg^{2+}-free HBSS and centrifuged at 300 × *g* for 5 min at 25 °C, and the pellet was resuspended in Neurobasal medium (Invitrogen) containing 5% donor horse serum (Invitrogen) and plated at ~70 cells/mm^2 on poly-L-lysine (100 μg/ml; 30,000–70,000 molecular weight)-coated coverslips (Carolina Biological Supply, Burlington, NC) for immunofluorescence experiments and at ~210 cells/mm^2 on 60-mm tissue culture dishes (600,000 cells/dish) for biochemical experiments. Growth medium consisted of Neurobasal medium supplemented with 0.5 mM L-glutamine, 10 mM HEPES, and NS21 supplement (22). Cytosine-D-arabinofuranoside (2.5 μM) was added 3 days after plating to reduce the number of non-neuronal cells. After 4 days in culture and once each week thereafter, half of the growth medium was replaced with medium without cytosine-D-arabinofuranoside. Neurons were transfected at 8 DIV using Lipofectamine 2000 (Invitrogen) for 2 h and used 2 days post-transfection, essentially as described previously (23).

Immunopurification by Immunoprecipitation—A crude rat brain membrane (RBM) fraction was prepared as described previously (21). Briefly, Sprague-Dawley rats were sacrificed by rapid decapitation, and the brains were removed and homogenized within a 1.5-min post-mortem period in homogenization buffer (5 mM sodium phosphate, pH 7.4, 320 mM sucrose, 100 mM NaF, 500 μM phenylmethylsulfonyl fluoride (PMSF), and a protease inhibitor mixture (2 μg/ml aprotinin, 2 μg/ml antipain, 1 μg/ml leupeptin, and 10 μg/ml benzamidine). Homogenates were centrifuged twice at 750 × *g* for 10 min at 4 °C. The supernatants were mixed and centrifuged at 38,000 × *g* for 90 min at 4 °C. One milligram of total RBM protein was solubilized in lysis buffer (1% (v/v) Triton X-100, 150 mM NaCl, 1 mM EDTA, 50 mM Tris-HCl (pH 7.4), 1 mM sodium orthovanadate, 5 mM NaF, 1 mM PMSF, and protease inhibitor mixture for 30 min at 4 °C, followed by centrifugation at 12,000 × *g* for 10 min at 4 °C. The supernatants were incubated with KC antibody overnight at 4 °C, followed by the addition of 50 μl of protein A-Sepharose beads (GE Healthcare) for 1 h at 4 °C. The beads were washed five times in lysis buffer and used for subsequent assays, or immunopurified proteins were eluted by boiling in 100 μl of reducing SDS sample buffer (RSB).

In Vitro Dephosphorylation Assay—Kv2.1 channels immunopurified from RBM by immunoprecipitation were dephosphorylated with 5 units of recombinant rabbit muscle PP1α (Calbiochem) in PP1 reaction buffer (50 mM Tris-HCl, pH 7.0, 5 mM DTT, 200 μM $MnCl_2$, 100 μM EDTA) for 1 h at 32 °C. The beads were washed once in lysis buffer, and the reaction was stopped by boiling in 100 μl of RSB.

In Vitro Phosphorylation Assay—A GST fusion protein (GST-MK1, 2.5 μg) containing the bulk (amino acids 509–853) of the Kv2.1 C terminus was incubated with 100 ng of recombinant human CDK5-p35 complex (Invitrogen) and 2 mM ATP in kinase reaction buffer (20 mM Tris-HCl, pH 7.5, 1 mM $MgCl_2$, 1 mM DTT) in a final volume of 50 μl for 15 min at 30 °C. The reaction was stopped by adding 50 μl of 2× RSB. For RBM reactions, 3 mg of RBM protein were treated with calf intestinal alkaline phosphatase (AP (0.1 unit/ml); Roche Applied Science) in AP reaction buffer (0.1% (w/v) SDS, 0.1 mM EDTA, 50 mM Tris-HCl, pH 8.5) in a final volume of 1.5 ml. NaF was added to 1 mM to the control reaction. The reactions were incubated for 2 h at 37 °C. Kv2.1 was purified from 1 mg of RBM (AP-treated and control) by immunoprecipitation using KC antibody overnight at 4 °C in 0.1% (w/v) SDS, 150 mM NaCl, 1 mM EDTA, 50 mM Tris-HCl (pH 7.4), 5 mM NaF, 1 mM PMSF, and protease inhibitor mixture. Immunocomplexes were recovered by incubation for 1 h at 4 °C with protein A-agarose beads. The beads were washed three times in kinase reaction buffer before use in the *in vitro* phosphorylation reaction as described above.

In Gel Digestion and LC-MS/MS Analysis—*In vitro* phosphorylation reaction products of GST-MK1 fusion protein were prepared and analyzed as described previously (15, 24). In brief, samples were separated by 12% SDS-PAGE, and the gel bands revealed by colloidal Coomassie Blue staining were excised from the gel; diced; washed twice in 50% acetonitrile, 25 mM ammonium bicarbonate; and dried for 10 min in a speed vacuum concentrator. Gel pieces were incubated in 10 mM DTT at 56 °C for 1 h to reduce Cys residues, which were then alkylated by incubation with 55 mM iodoacetamide at room temperature for 45 min in the dark. Gel pieces were then washed 10 min in 50 mM ammonium bicarbonate; dehydrated in 50% acetonitrile, 50 mM ammonium bicarbonate for 10 min; and dried in a vacuum concentrator. Dried gel pieces were rehydrated with 100 μl of 50 mM ammonium bicarbonate on ice for 10 min, and this solution was replaced with 50 mM ammonium bicarbonate containing 10 ng/μl trypsin (Promega, Valencia, CA), followed by overnight incubation at 37 °C. Digested peptides were extracted by vortexing with 50% acetonitrile, 5% formic acid for 30 min, and the extracts were completely dried in a vacuum concentrator until analysis. LC-MS/MS procedures were performed at the University of California Davis Proteomics Facility using an ultraperformance liquid chromatography system (nanoACQUITY, Waters, Milford, MA) coupled with an ion trap mass spectrometer (LTQ-FT, Finnigan, San Jose, CA) for LC-MS/MS data acquisition. MS/MS spectra were interpreted through Mascot searches (Matrix Science, Westminster, UK) with a mass tolerance of 20 ppm, MS/MS tolerance of 0.4 or 0.6 Da, and one missed cleavage site allowed. Carbamidomethylation of cysteine; oxidation of methionine; and

phosphorylation on serine, threonine, and tyrosine residues was allowed. Each filtered MS/MS spectrum exhibiting possible phosphorylation was manually checked and validated. The existence of a 98-Da mass loss (-H_3PO_4; phosphopeptide-specific CID neutral loss) and any ambiguity of phosphosites were carefully examined.

Kainate-induced Seizure Animals—All animal use procedures were in strict accordance with the National Institutes of Health Guide for the Care and Use of Laboratory Animals and were approved by the Institutional Animal Care and Use Committee of the University of California Davis. Adult (250 g) male rats were injected with 10 mg/kg kainic acid (K0250, Sigma) dissolved in PBS or with PBS alone. The progression of seizure after injection was assessed according to Racine's classification (25). A full behavioral seizure, with loss of postural control, was considered as a class 5 motor seizure or status epilepticus. Animals were killed by decapitation 2 h after the initial seizure onset (typically 10–20 min after injection) and after remaining in status epilepticus for at least 20 min prior to decapitation. Pentobarbital (60 mg/kg) was given to a subset of animals 5 min before decapitation.

Immunoblot Analysis and Quantification—Transfected HEK293 cells were washed once with ice-cold DPBS and lysed with 150 μl of ice-cold lysis buffer containing 1% (v/v) Triton X-100, 150 mM NaCl, 1 mM EDTA, 50 mM Tris-HCl (pH 7.4), 1 mM sodium orthovanadate, 5 mM NaF, 1 mM PMSF, and protease inhibitor mixture for 10 min at 4 °C. The lysates were centrifuged at 12,000 × *g* at 4 °C for 10 min. The supernatants were mixed with 150 μl of 2× RSB and size-fractionated by 7.5% SDS-PAGE. Lauryl sulfate (L-5750, Sigma) was the form of SDS used in all gel solutions (20). For biochemical experiments, neuronal cultures were stimulated at 37 °C in 1× HBSS for the appropriate time. After the incubation, cells were washed once and harvested in 1 ml of ice-cold Locke's solution (154.0 mM NaCl, 5.6 mM KCl, 2.3 mM $CaCl_2$, 1.0 mM $MgCl_2$, 5.0 mM glucose, 5.0 mM HEPES, pH 7.4) and centrifuged at 11,000 × *g* at 4 °C for 3 min, and the cell pellet was lysed in 100 μl of RSB, heated at 95 °C for 5 min, and size-fractionated by 7.5% SDS-PAGE. Following SDS-PAGE, proteins were transferred to nitrocellulose membranes (Bio-Rad), which were blocked for 1 h with Blotto (3% (w/v) nonfat milk, 0.1% (v/v) Tween 20 in Tris-buffered saline (TBS; 50 mM Tris, pH 7.5, 150 mM NaCl) followed by 2-h or overnight incubation with primary antibodies. After three washes with Blotto, the membranes were incubated with the appropriate HRP-conjugated secondary antibody for 1 h. After three washes with 0.1% (v/v) Tween 20, TBS, the immunoblots were visualized by Pierce ECL Western blotting substrate (Thermo Scientific, Rockford, IL) in a FluorChem Q imager (Cell Biosciences, Santa Clara, CA) and quantified using National Institutes of Health ImageJ software.

Immunofluorescence Staining—Cultured hippocampal neurons (15–21 DIV) that had been subjected to various treatments were fixed for 15 min at 4 °C in 4% formaldehyde, 4% sucrose in DPBS and washed in DPBS. Neurons were permeabilized and blocked with 0.1% Triton X-100, 3% (w/v) nonfat dry milk in DPBS for 45 min at room temperature and stained with anti-Kv2.1 mouse K89/34 mAb and rabbit anti-MAP2 polyclonal antibody. Primary antibodies were detected with Alexa 488 goat anti-mouse IgG1 and Alexa 594 goat anti-rabbit or with Alexa 594 goat anti-mouse IgG1 and Alexa 350 goat anti-rabbit secondary antibodies (Invitrogen). Images were acquired with a CCD camera installed on an Axiovert 200M microscope with ×63, 1.3 numerical aperture objective and an ApoTome coupled to Axiovision software (Zeiss, Oberkochen, Germany). Kv2.1 clustering was quantified by converting the original images to binary images using a fixed threshold, and spots corresponding to Kv2.1 clusters were measured and counted using National Institutes of Health Image J software.

Statistical Analyses—All data are expressed as the mean ± S.D. Normalized data were compared with respective controls using a two-way analysis of variance and *post hoc* Dunnett's test, except for data in Fig. 2*A*, which used an unpaired *t* test, and Fig. 2*C*, which used a one-way analysis of variance and *post hoc* Tukey test (all performed using Prism 4.0 (GraphPad, San Diego, CA)).

RESULTS

CDK5 Phosphorylates Kv2.1 in Heterologous Expression Systems—Bioinformatics analysis of the rat Kv2.1 primary sequence reveals that nine of the 16 phosphorylation sites identified on Kv2.1 purified from rat brain (15) are consensus sites for Pro-directed protein kinases, including CDK5 (Fig. 1*A*). To begin to address the PKs responsible for phosphorylating Kv2.1, we co-expressed recombinant Kv2.1 with a panel of recombinant PKs in HEK293 cells. Co-transfection of Kv2.1 with plasmids encoding WT CDK5 and p35 cofactor led to expression of Kv2.1 with a slightly decreased electrophoretic mobility (Fig. 1*B*), consistent with enhanced overall phosphorylation (note the mobility shift of Kv2.1 in control lanes of RBM ± AP treatment) and a significant increase (2.35 ± 0.65-fold, $p < 0.05$, $n = 3$) in the immunoreactivity of Kv2.1 with a phosphospecific antibody, pS603 (7, 15), specific for phosphorylation at Ser-603 (Fig. 1*B*), a site that is key to phosphorylation-dependent regulation of Kv2.1 gating (15). Co-expression of Kv2.1 with p35 and a dominant-negative version of CDK5 (CDK5-DN) containing an Asn substitution at Asp-144 or with p35 alone did not significantly affect Kv2.1 phosphorylation (Fig. 1*B*). These results suggest, as predicted from the bioinformatics analyses, that Kv2.1 may be a substrate for the CDK5-p35 complex. However, it is also possible that CDK5 overexpression plays an indirect role in increasing Kv2.1 phosphorylation by regulating other PKs and/or PPs that then directly determine the Kv2.1 phosphorylation state.

CDK5 Directly Phosphorylates Kv2.1—To address whether Kv2.1 is a direct substrate of CDK5-p35, we performed *in vitro* phosphorylation reactions using purified recombinant human CDK5-p35 complex and a bacterially expressed recombinant GST fusion protein containing a fragment of the Kv2.1 cytoplasmic C terminus corresponding to amino acids 509–853, which contains a total of 49 Ser and 24 Thr residues, and 11 of the sites (Fig. 1*B*) identified in our previous analysis of *in vivo* Kv2.1 phosphorylation sites (15). The reaction products were analyzed by immunoblot with the pS603 antibody, which revealed a lack of detectable phosphorylation on the bacterially expressed fragment in the control reaction performed without PK but a robust pS603 signal in the sample subjected to *in vitro* phosphorylation with the CDK5-p35 complex (Fig. 2*A*). A par-

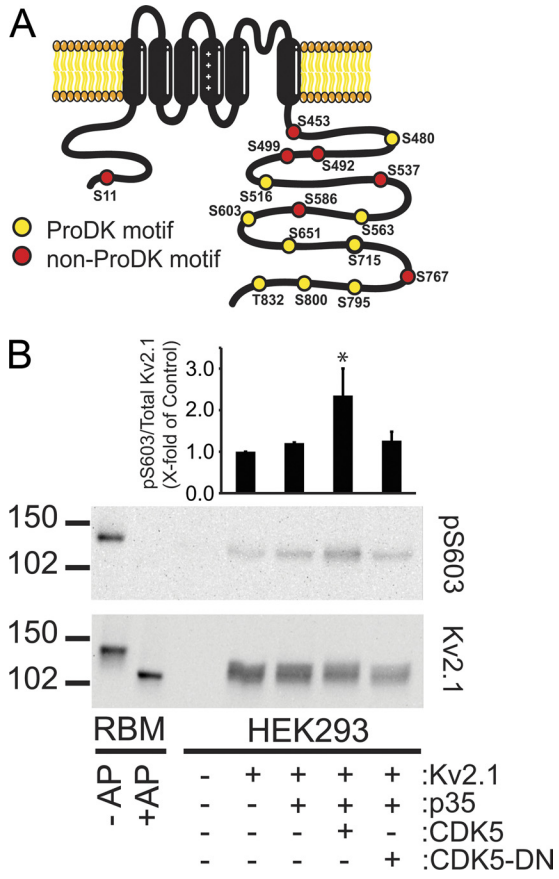

FIGURE 1. **CDK5 co-expression leads to enhanced Kv2.1 phosphorylation in HEK293 cells.** *A*, schematic representation of the location of previously identified *in vivo* Kv2.1 phosphorylation sites. *Colors* depict those that do (*yellow symbols*) and do not (*red symbols*) conform to consensus sites for Pro-directed kinases (*ProDKs*). *B*, analysis of Kv2.1 phosphorylation in HEK293 cells. Cells were transiently transfected with plasmids encoding Kv2.1, CDK5, dominant-negative CDK5-D144N (*DN*), and CDK5 cofactor p35, as labeled *below* the *immunoblot lanes*. Transfected cell extracts were analyzed by immunoblotting for Kv2.1 phosphorylated at Ser-603 (pS603) and for total Kv2.1. *Numbers* to the *left* of blots indicate the mobility of molecular mass standards in kDa. RBM preparations without or with prior AP treatment (−/+ *AP*) were analyzed as control samples containing phosphorylated and dephosphorylated Kv2.1, respectively. The *bar graph above* the *immunoblot lanes* shows quantitation of immunoblot signals from three independent experiments. *, significant difference ($p < 0.05$) from control.

allel immunoblot with a general anti-Kv2.1 antibody revealed a small shift in the electrophoretic mobility of Kv2.1 in the CDK5-p35 reaction, indicative of enhanced overall phosphorylation (Fig. 2*A*).

The products of these *in vitro* phosphorylation reactions were next analyzed by LC-MS/MS to independently confirm phosphorylation at Ser-603 and to determine whether other Kv2.1 sites were also CDK5-p35 substrates. These analyses yielded extensive sequence coverage but did not identify any detectable phosphorylation on the bacterially expressed Kv2.1 fragment from the control reaction (data not shown). However, the sample subjected to *in vitro* phosphorylation with CDK5-p35 complex contained tryptic phosphopeptides in which phosphorylation could be unambiguously assigned to Ser-516 (SSSpSPQHLNVQQLEDMYSK (where pS represents phosphoserine), Mascot score 47), Ser-603 (FSHpSPLASLSSK, Mascot score 54), Ser-651 (SGFFVEpSPR, Mascot score 53), and Ser-800 (TEKNHFESSPLPTpSPK, Mascot score 53; NHFESSPLPTpSPK, Mascot score 34). Fig. 2*B* shows the tandem mass spectrum for the phosphopeptide FSHpSPLASLSSK (amino acids 600–611) that was used to assign phosphorylation to Ser-603. These four sites were predicted by software algorithms as consensus CDK5 phosphorylation sites (Fig. 1*A*). Moreover, each of these sites had been previously identified as phosphosites on Kv2.1 in the brain and from Kv2.1 expressed in HEK293 cells (15, 16, 26, 27), suggesting that phosphorylation at these sites *in vivo* is mediated by CDK5.

To determine whether CDK5-p35 could directly phosphorylate native brain Kv2.1 protein, we next performed *in vitro* phosphorylation assays using purified CDK5-p35 complex and Kv2.1 immunopurified from rat brain as the substrate. Reactions were performed on Kv2.1 purified from brain samples prepared without and with pretreatment with AP to remove preexisting *in vivo* phosphorylation. In these experiments, we found that, consistent with our previous studies (7), a subpopulation of Kv2.1 in rat brain Kv2.1 was already phosphorylated at Ser-603 *in vivo*. However, *in vitro* phosphorylation with CDK5-p35 yielded increased Kv2.1 phosphorylation at Ser-603 (Fig. 2*C*), consistent with our previous results that showed that Kv2.1 in control RBM samples was not maximally phosphorylated at this site (7). Treatment with AP led to a dramatic increase in Kv2.1 electrophoretic mobility on SDS gels, indicative of effective overall dephosphorylation of Kv2.1, and removed all detectable Ser-603 phosphorylation (Fig. 2*C*). *In vitro* phosphorylation of this dephosphorylated brain Kv2.1 sample with CDK5-p35 partially restored phosphorylation at Ser-603 and also yielded a slight decrease in the electrophoretic mobility of Kv2.1 (Fig. 2*C*), similar to that observed upon *in vitro* phosphorylation of the recombinant Kv2.1 fragment in Fig. 2*A*. These results suggest that Kv2.1 is a direct substrate for phosphorylation by CDK5-p35 at a subset of the known *in vivo* phosphorylation sites and that Ser-603 is among these.

Effects of Inhibiting CDK5 on Neuronal Kv2.1 Phosphorylation and Localization—To determine the impact of CDK5-mediated phosphorylation on neuronal Kv2.1, we investigated the effects of pharmacologically inhibiting CDK5 in cultured hippocampal neurons with roscovitine. Although roscovitine at the concentration used here (10 μM) inhibits CDK1, CDK2, and CDK5, previous studies have shown that among these CDKs, only CDK5 is present in hippocampal neurons (28). Note that roscovitine (at 30 μM) is a direct inhibitor of Kv2.1 channels, through a mechanism that involves open channel block (29). However, previous studies suggest that, in itself, blocking Kv2.1 channels in hippocampal neurons does not lead to altered Kv2.1 phosphorylation (13).

To determine the effect of CDK5 inhibition on Kv2.1 localization, we treated 15 DIV hippocampal neuronal cultures with 10 μM roscovitine for 1 h. As in brain neurons, Kv2.1 exhibits robust clustering in hippocampal neurons in culture (23), where clustering is dependent on maintenance of Kv2.1 phosphorylation (5). We observed that control neurons exhibited robust clustering of Kv2.1, whereas neurons in the roscovitine-treated samples had lost these obvious Kv2.1 clusters and instead expressed Kv2.1 with a diffuse localization (Fig. 3*A*). Overall, the number of Kv2.1 clusters per cell was significantly reduced by roscovitine treatment (Fig. 3*B*; untreated, 19.26 ±

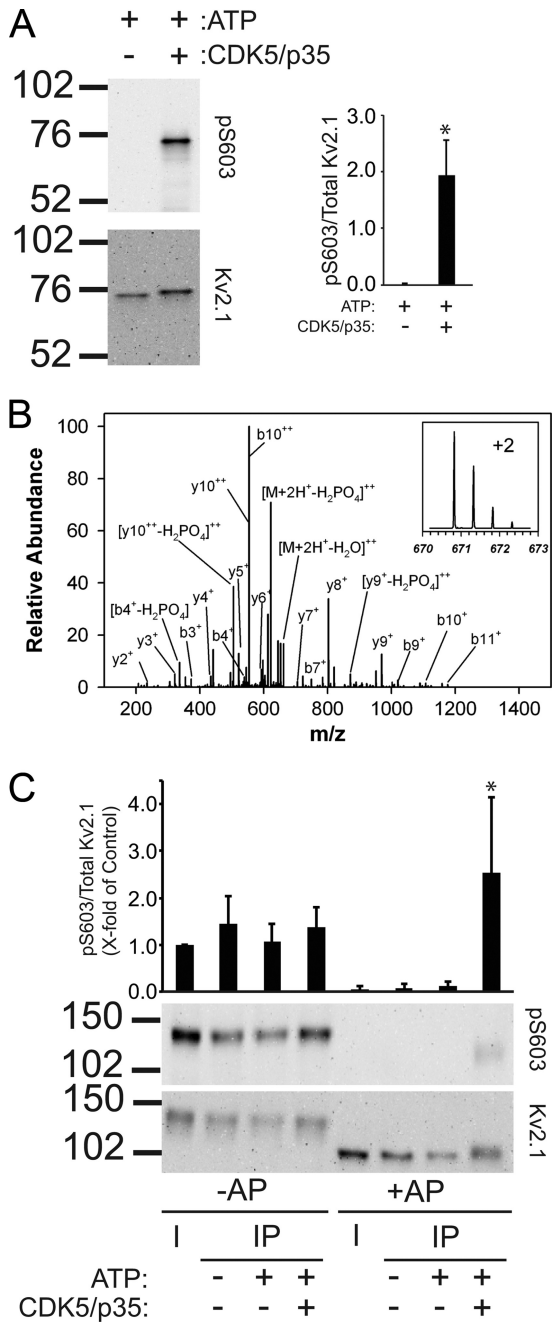

FIGURE 2. **CDK5 directly phosphorylates Kv2.1.** *A*, the Kv2.1 C terminus is phosphorylated by CDK5. A bacterially expressed GST fusion protein containing amino acids 509–853 of Kv2.1 was subjected to *in vitro* phosphorylation reactions without and with purified recombinant CDK5-p35 complex. Reactions were analyzed by immunoblot for Kv2.1 phosphorylated at Ser-603 (pS603) and total Kv2.1. The *right graph* shows quantitation of immunoblot signals from three independent experiments. *, significant difference ($p < 0.05$) from control. *B*, representative MS/MS spectrum of the Kv2.1 phosphopeptide ^{600}FSH[pS]PLASLSSK^{611} from the CDK5-p35 *in vitro* phosphorylation reaction exhibiting phosphorylation at Ser-603. *C*, CDK5-p35 phosphorylates Kv2.1 purified from rat brain. Kv2.1 was immunopurified from RBM without (−*AP*) or with (+*AP*) prior to AP digestion to remove preexisting *in vivo* phosphorylation and subjected to *in vitro* phosphorylation with CDK5-p35. *I*, RBM input; *IP*, immunopurified Kv2.1, subjected to *in vitro* phosphorylation without and with ATP and CDK5-p35, as noted *above* the *immunoblot lanes*. Reactions were analyzed by immunoblot for Kv2.1 phosphorylated at Ser-603 (pS603) and total Kv2.1. *Numbers* to the *left* of blots in *A* and *C* indicate the mobility of molecular weight standards in kDa. The *bar graph above* the *immunoblot lanes* shows quantitation of immunoblot signals from three independent experiments. *, significant difference ($p < 0.05$) from control reactions (+*AP*, −/+*ATP*, -*CDK5/p35*).

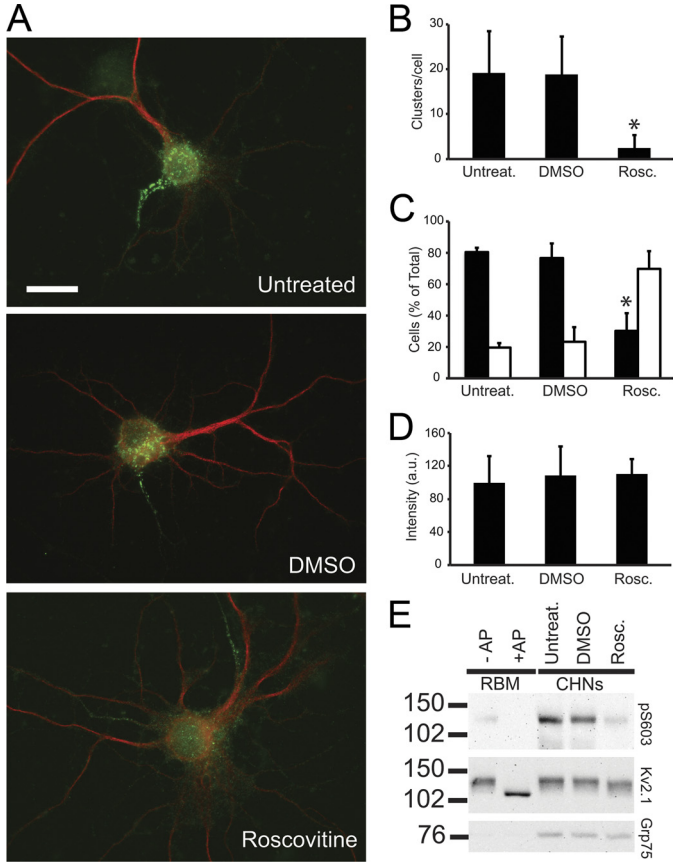

FIGURE 3. **Inhibiting CDK5 in neurons reduces both phosphorylation-dependent clustering and phosphorylation of Kv2.1.** *A*, representative images showing that inhibition of CDK5 in hippocampal neurons leads to disruption of Kv2.1 clustering. Cultured rat hippocampal neurons (15 DIV) were left untreated or treated with DMSO vehicle or 10 μM roscovitine for 1 h, fixed, and subjected to double immunofluorescence staining for Kv2.1 (*green*) and MAP2 (*red*). *Scale bar*, 20 μm. *B*, graph shows quantitation for number of clusters (area >0.7 μm^2) observed in each condition. *, significant differences ($p < 0.01$) *versus* both untreated and DMSO controls ($n = 20$ in each condition). *C*, *graph* shows data on percentage of neurons with (*black bars*) and without (*white bars*) clustering. Data are from eight independent coverslips from four independent experiments. *, significant difference ($p < 0.05$) *versus* untreated and DMSO controls. *D*, integrated fluorescence intensities of Kv2.1 immunolabeling. Intensities are expressed as a percentage of the fluorescence intensity in untreated cells (untreated, $n = 25$; DMSO, $n = 30$; roscovitine, $n = 40$). *E*, cultured rat hippocampal neurons (*CHNs*; 15 DIV) were left untreated (*Untreat.*) or treated with DMSO vehicle or 10 μM roscovitine (*Rosc.*) for 1 h, harvested, and analyzed by immunoblot for Kv2.1 phosphorylated at Ser-603 (pS603), total Kv2.1, or loading control Grp75. RBM preparations without or with prior AP treatment (−/+ *AP*) were analyzed as control samples containing phosphorylated and dephosphorylated Kv2.1, respectively. *Numbers* to the *left* of the blots indicate the mobility of molecular mass standards in kDa.

9.2; DMSO, 18.83 ± 8.52; roscovitine, 2.53 ± 2.82; 20 cells/condition; roscovitine $p < 0.01$ *versus* both untreated and DMSO-treated). The number of cells with obvious Kv2.1 clusters also dropped significantly, from 80.45 ± 2.75% in the untreated samples to 30.22 ± 11.32% following roscovitine treatment (Fig. 3*C*; $n = 4$ independent experiments of 100 cells each, $p < 0.05$; DMSO vehicle-treated samples had a value of 76.68 ± 9.31%). Note that no significant differences were observed in the total Kv2.1 fluorescence intensities in neurons subjected to the different treatments (Fig. 3*D*). These results together demonstrate that inhibition of CDK5 reduces the steady-state level of Kv2.1 clustering but not expression in

hippocampal neurons, probably due to decreased Kv2.1 phosphorylation.

We found that roscovitine treatment of cultured hippocampal neurons also leads to a loss of pS603 signal on immunoblots as well as a slightly increased electrophoretic mobility of the total Kv2.1 pool, consistent with a reduction in overall phosphorylation state (Fig. 3*E*). These data together suggest that CDK5 phosphorylation contributes to maintaining the level of steady-state Kv2.1 phosphorylation in hippocampal neurons.

CDK5 Mediates the Rapid Phosphorylation of Neuronal Kv2.1 upon Acute Activity Blockade—Kv2.1 phosphorylation exhibits bidirectional regulation *in vivo*, such that enhanced neuronal activity associated with kainate-induced seizures lead to extensive dephosphorylation (5, 7), whereas reducing neuronal activity *in vivo* with anesthetics, such as pentobarbital, leads to enhanced phosphorylation of Kv2.1 (7). Here we determined whether acute pentobarbital treatment could reverse the effects of hyperactivity associated with kainate-induced status epilepticus on Kv2.1 phosphorylation state. Rats were subjected to status epilepticus (Racine scale five) for 2 h total, with a final seizure of at least 20-min duration, to induce robust Kv2.1 dephosphorylation, and then a subset was subsequently treated with pentobarbital for 5 min. A subset of control animals was also treated with pentobarbital for 5 min. As shown in Fig. 4*A* and as previously reported (5, 7), Kv2.1 from an animal in status epilepticus had increased electrophoretic mobility consistent with a reduction in overall phosphorylation and loss of phosphorylation at Ser-603. However, brief (5-min) treatment with pentobarbital completely reversed the robust effects of the kainate-induced status epilepticus, suggesting that acute and brief suppression of neuronal activity, even following prolonged periods of kainate-induced status epilepticus, could trigger enhanced Kv2.1 phosphorylation.

These results led us to question whether acute activity blockade in cultured neurons would also trigger enhanced Kv2.1 phosphorylation. We treated neurons for 15 min with TTX and found that this acute activity blockade also leads to increased Kv2.1 phosphorylation at Ser-603 (Fig. 4*B*, compare *control lanes −/+ TTX*). To determine whether CDK5 plays a role in the rapid hyperphosphorylation of Kv2.1 observed upon acute activity blockade, we treated cultured rat hippocampal neurons with roscovitine prior to TTX treatment. We observed that, similar to the results shown in Fig. 3*E*, CDK5 inhibition in the absence of TTX leads to diminished Kv2.1 phosphorylation at Ser-603, in this case by 60% (Fig. 4*B*). Whereas TTX treatment causes a rapid ~3-fold increase in the phosphorylation of Ser-603 in the absence of roscovitine, pharmacological CDK5 inhibition prevented the TTX-induced increase in Ser-603 phosphorylation (Fig. 4*B*). These results suggest that CDK5 mediates not only the constitutive phosphorylation of Kv2.1 but also the rapid increase in Kv2.1 phosphorylation in response to acute blockade of neuronal activity.

CDK5 Activity Contributes to the Recovery of Phosphorylation of Kv2.1 Channel after Excitatory Stimulation—Our previous studies showed that increased neuronal activity leads to a dephosphorylation and unclustering of Kv2.1, followed by the subsequent recovery over a 2-h time frame (5). Interestingly, CDK5 activity is also diminished after glutamate treatment due

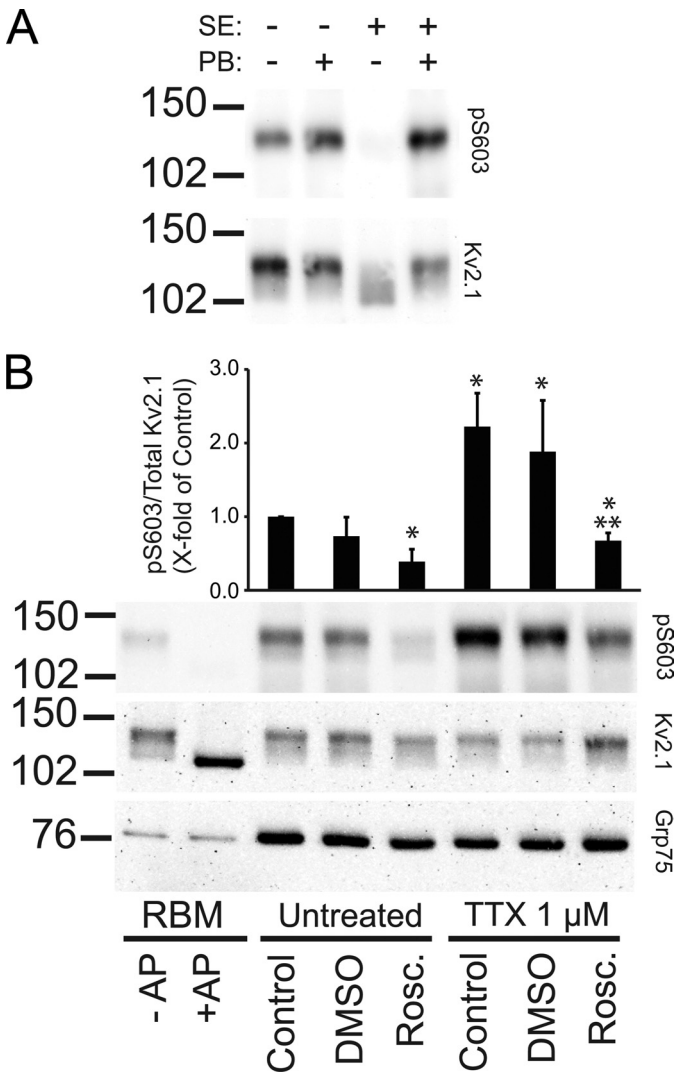

FIGURE 4. **Acute activity blockade triggers rapid Kv2.1 phosphorylation.** *A*, pentobarbital treatment causes a rapid reversal of the effects of status epilepticus on Kv2.1 phosphorylation *in vivo*. RBMs were prepared from control rats or rats subjected to kainate-induced status epilepticus (*SE*) for 2 h, without or with a subsequent 5-min treatment with pentobarbital (*PB*) before decapitation. Samples were analyzed by immunoblot for Kv2.1 phosphorylated at Ser-603 (pS603) and total Kv2.1. *B*, inhibiting CDK5 abolishes the homeostatic increase in Kv2.1 phosphorylation in response to acute activity blockade in cultured neurons. Cultured rat hippocampal neurons were treated with DMSO vehicle or 10 μM roscovitine for 45 min and then with 1 μM TTX for 15 min in the same solutions, as detailed *below* the *immunoblot lanes*. Neurons were analyzed by immunoblot for Kv2.1 phosphorylated at Ser-603 (pS603) and total Kv2.1, and for loading control Grp75. RBM preparations without or with AP treatment (*−/+ AP*) were analyzed as control samples containing phosphorylated and dephosphorylated Kv2.1, respectively. The *bar graph above* the *immunoblot lanes* shows quantitation of immunoblot signals from three independent experiments. Shown are samples with a signal significantly different ($p < 0.05$) from untreated control (*) or TTX control (**). *Numbers* to the *left* of both *panels* indicate the mobility of molecular mass standards in kDa.

to degradation of its p35 cofactor, and recovery of CDK5 activity after glutamate washout (30, 31) occurs with a time course similar to Kv2.1 rephosphorylation. Given the results above demonstrating an important role for CDK5 in the steady-state phosphorylation of Kv2.1, and in mediating the enhanced phosphorylation of Kv2.1 upon activity blockade, we next investigated the role of CDK5 in the recovery of Kv2.1 phosphorylation after excitation-induced dephosphorylation. We stimulated neu-

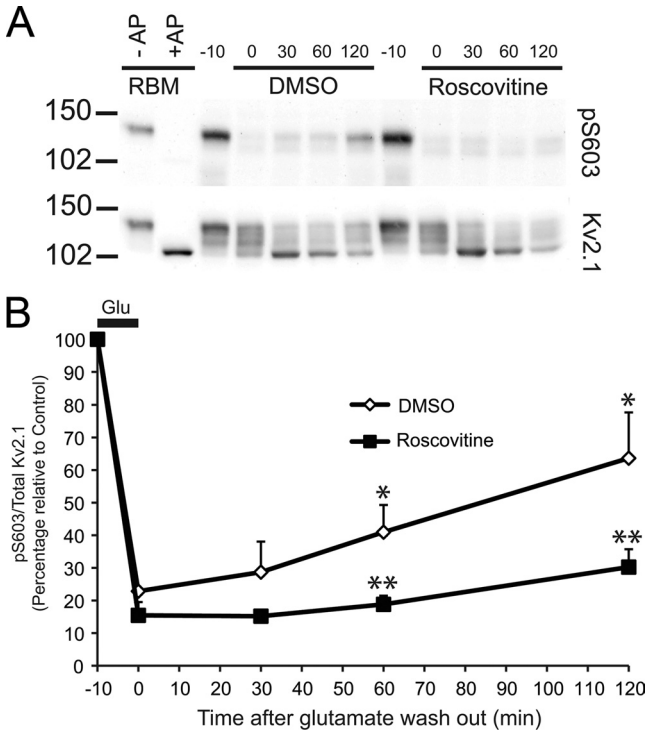

FIGURE 5. **Inhibiting CDK5 prevents the recovery of Kv2.1 phosphorylation following glutamate-induced dephosphorylation.** *A*, cultured rat hippocampal neurons were treated with 10 μM glutamate for 10 min in HBSS. The solution was replaced by complete medium with DMSO vehicle or 10 μM roscovitine. Neurons before (−10 min) and at different times after glutamate treatment, as *labeled above* the *lanes*, were harvested and analyzed by immunoblot for Kv2.1 phosphorylated at Ser-603 (pS603) and total Kv2.1. RBM preparations without or with AP treatment (*−/+ AP*) were analyzed as control samples containing phosphorylated and dephosphorylated Kv2.1, respectively. *Numbers* to the *left* indicate the mobility of molecular mass standards in kDa. *B*, graph shows quantitation of immunoblot signals from three independent experiments. Shown are DMSO control samples at time points that are significantly different ($p < 0.05$) from the time 0 DMSO control sample (*) or roscovitine samples that are significantly different ($p < 0.05$) from DMSO controls at the same time point (**).

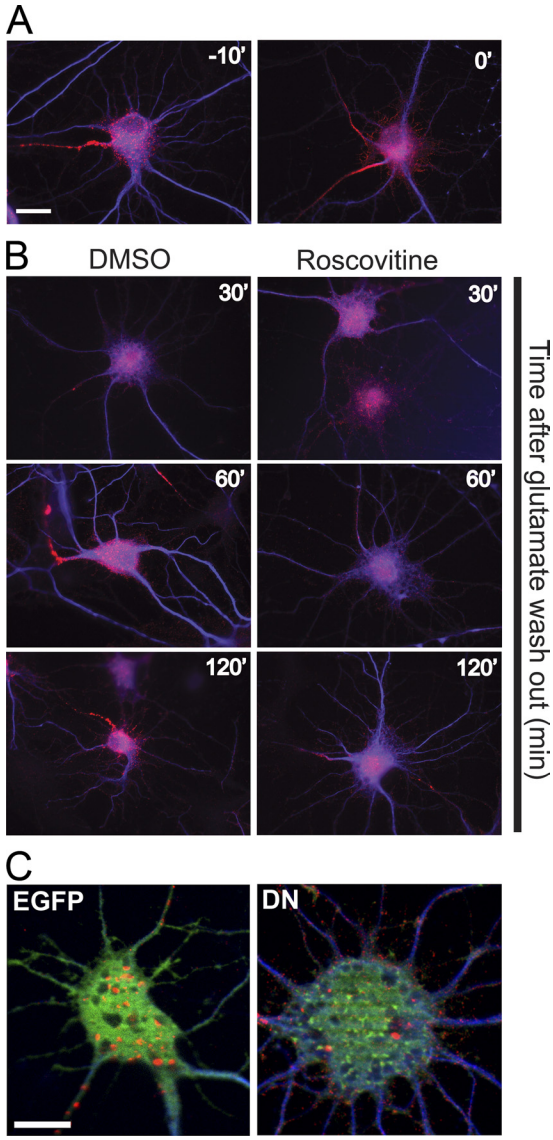

FIGURE 6. **Inhibiting CDK5 prevents the recovery of Kv2.1 clustering following glutamate-induced dephosphorylation.** *A*, immunofluorescence staining showing the disruption of somatic Kv2.1 clusters by glutamate. *B*, CDK5-dependent recovery of clustering after glutamate washout. Neurons treated as in Fig. 5 were fixed and stained for Kv2.1 (*red*) and MAP-2 (*blue*). *Scale bar*, 20 μm. *C*, GFP-CDK5-D144N (*DN*) expression disrupts the recovery of Kv2.1 clustering after glutamate treatment. Neurons transfected with EGFP (*green*) or GFP-CDK5-D144N (*green*) and treated as in *A* were fixed and stained for Kv2.1 (*red*) and MAP-2 (*blue*). *Scale bar*, 10 μm.

rons with 10 μM glutamate for 15 min and then washed out the glutamate and followed the time course of Kv2.1 recovery up to 120 min under control and roscovitine-treated conditions. We observed a slow recovery of Kv2.1 phosphorylation, similar to that described previously (5) under control conditions (DMSO), such that Ser-603 phosphorylation had recovered to 63.6 ± 14.0% of the level seen in unstimulated neurons after 120 min of recovery (Fig. 5, *A* and *B*). However, significantly less recovery of Ser-603 phosphorylation (to 30.2 ± 5.5 of unstimulated levels after 120 min of recovery) was observed when roscovitine was present during the recovery period (Fig. 5, *A* and *B*). In addition, roscovitine treatment reduced the number of neurons exhibiting clusters after a 120-min washout time (74.3 ± 8.5% of neurons exhibiting clusters in DMSO-treated *versus* 2.6 ± 1.4% of neurons exhibiting clusters with roscovitine treatment; Fig. 6*B*). Moreover, molecular inhibition of CDK5 activity using transfection with CDK5-D144N (*DN*) also inhibited recovery of Kv2.1 clustering after excitation-induced declustering (Fig. 6*C*). Together, these results suggest that CDK5 plays a crucial role in the rephosphorylation of Kv2.1 that is required for recovery of clustering following an excitatory stimulus.

The Role of Protein Phosphatase PP1 in Regulating Kv2.1 Phosphorylation—Our previous studies (5) suggested that PP1 contributes to the maintenance of constitutive phosphorylation of Kv2.1 in control neurons but does not participate in rapid dephosphorylation of Kv2.1 in response to excitatory stimuli (mediated instead by calcineurin). To determine whether Kv2.1 was a direct substrate for PP1, we performed an *in vitro* dephosphorylation assay using purified recombinant PP1 protein and Kv2.1 immunopurified from rat brain. As shown in Fig. 7*A*, incubation of Kv2.1 with PP1 results in loss of all detectable phosphorylation at Ser-603, similar to that observed upon *in vitro* AP treatment. Treatment with PP1 also caused a shift in the electrophoretic mobility of Kv2.1 on SDS gels, although not to the same extent as AP treatment (Fig. 7*A*).

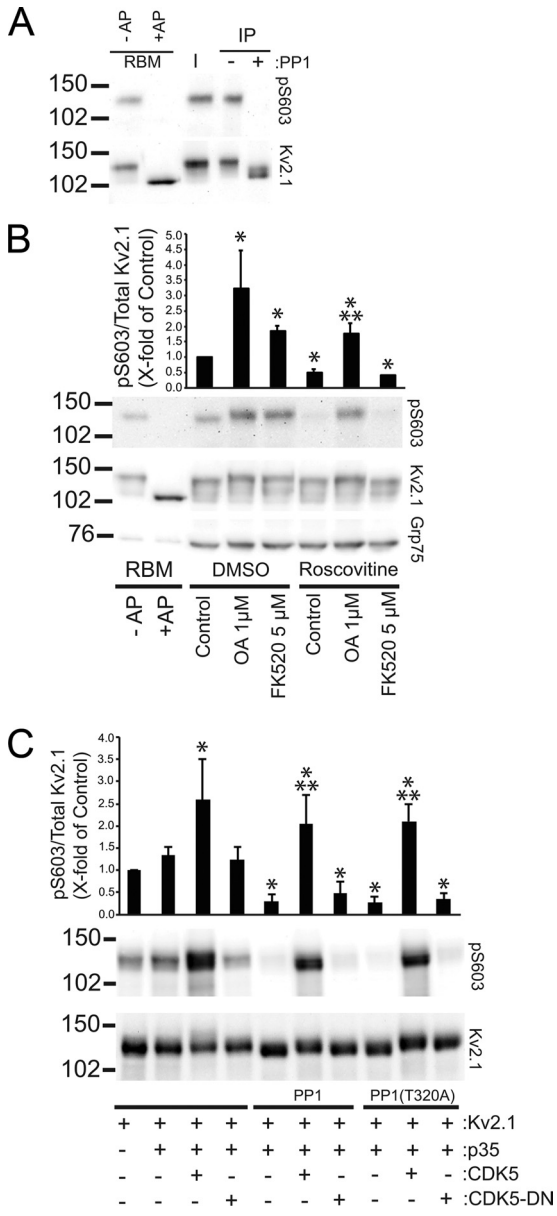

FIGURE 7. **CDK5 and PP1 work in concert to control the steady-state phosphorylation of Kv2.1.** *A*, Kv2.1 is a substrate for PP1. Kv2.1 immunopurified from rat brain was subjected to *in vitro* dephosphorylation using purified PP1. The immunoblot shows RBM input (*I*) and immunopurified Kv2.1, subjected to *in vitro* dephosphorylation reactions without and with PP1 (*IP*). Reactions were analyzed by immunoblot for Kv2.1 phosphorylated at Ser-603 (pS603) and total Kv2.1. *B*, inhibiting CDK5 prevents increased Kv2.1 phosphorylation induced by inhibition of protein phosphatases. Hippocampal neurons in culture were treated with vehicle DMSO or 10 μM roscovitine for 50 min and then treated with phosphatase the inhibitor okadaic acid (for PP1 and PP2A) or FK520 (for PP2B/calcineurin) for 10 min in the same solutions. Neurons were harvested and analyzed by immunoblot for Kv2.1 phosphorylated at Ser-603 (pS603) and total Kv2.1 and for loading control Grp75. The *bar graph above* the *immunoblot lanes* shows quantitation of immunoblot signals from three independent experiments. Shown are samples with a signal significantly different ($p < 0.05$) from DMSO control (*) or roscovitine-treated (**). *C*, PP1 co-expression leads to reduced Kv2.1 phosphorylation in HEK293 cells. HEK293 cells were transiently transfected with Kv2.1, WT PP1, or a PP1 mutant refractory to regulation by CDK5 (PP1(T320A)), together with GFP-CDK5, dominant-negative GFP-CDK5-D144N (*DN*), and CDK5 cofactor p35, as denoted *below* the *immunoblot lanes*. Cells were harvested 48 h post-transfection and analyzed by immunoblot for Kv2.1 phosphorylated at Ser-603 (pS603) and total Kv2.1. The *bar graph above* the *immunoblot lanes* shows quantitation of immunoblot signals from three independent experiments. Shown are samples with a signal significantly different ($p < 0.05$) from Kv2.1 alone (*) or from PP1 or PP1(T320A) (**). Immunoblots in *A* and *B* contain RBM preparations without or with prior AP treatment (−/+ *AP*) as control samples containing phosphorylated and dephosphorylated Kv2.1, respectively. *Numbers* to the *left* of all *panels* indicate the mobility of molecular mass standards in kDa.

This suggests that some but not all of the steady-state phosphorylation present on Kv2.1 in rat brain is sensitive to direct dephosphorylation by PP1, including phosphorylation at Ser-603.

Given these results, we next determined whether PP1 activity contributed to the decreased level of Kv2.1 phosphorylation observed upon CDK5 inhibition. We treated neurons with roscovitine for 1 h to inhibit CDK5, followed by a 10-min treatment with either 1 μM okadaic acid (a PP1 and PP2A inhibitor) or FK520 (a PP2B/calcineurin inhibitor). We found that, consistent with previous results (5), okadaic acid treatment increased the overall steady-state level of Kv2.1 phosphorylation in control neurons, as indicated by a shift in the electrophoretic mobility of Kv2.1 (Fig. 7*B*). Moreover, okadaic acid treatment induced a 3.24 ± 1.23-fold ($n = 3$) increase in phosphorylation of Kv2.1 at Ser-603 (Fig. 7*B*). In addition, we found that okadaic acid treatment abolished the roscovitine effects on Kv2.1 phosphorylation (1.76 ± 0.33 relative to control DMSO, $n = 3$). These results suggest that constitutive levels of Kv2.1 phosphorylation are maintained through concerted activity of CDK5 and PP1 and that, upon inhibition of CDK5, constitutive PP1 activity drives Kv2.1 into a dephosphorylated state.

CDK5 plays a crucial role as a negative regulator of PP1 activity. CDK5 phosphorylation of a key regulatory site (Thr-320) on PP1 itself inhibits PP1 activity (32, 33). Given these inhibitory effects of CDK5 on PP1 activity, it is possible that some or all of the effects of CDK5 inhibition by roscovitine could be mediated indirectly by increased PP1 activity and not via decreased CDK5 phosphorylation of Kv2.1. To determine whether any of the effects of manipulating CDK5 activity on Kv2.1 phosphorylation are mediated through PP1, we investigated the level of Kv2.1 phosphorylation in HEK293 cells co-expressing Kv2.1 and CDK5-p35, together with either WT PP1 or the PP1(T320A) mutant that is refractory to CDK5-dependent inhibition. We found that co-expression of Kv2.1 with either PP1 or PP1(T320A) yielded an altered electrophoretic mobility of Kv2.1 indicative of overall dephosphorylation and a 3.3-fold reduction in phosphorylation at Ser-603 (0.30 ± 0.17 and 0.27 ± 0.14 relative to control, respectively; Fig. 7*C*). However, co-expression of CDK5-p35 with either PP1 or PP1(T320A) yielded levels of Kv2.1 phosphorylation comparable with those observed with CDK5-p35 alone (Fig. 7*C*). These results suggest that although PP1 contributes to the steady-state levels of Kv2.1 phosphorylation, the primary role of CDK5 in determining the phosphorylation state of Kv2.1 is via direct phosphorylation of Kv2.1, as opposed to CDK5-mediated inactivation of PP1.

DISCUSSION

Plasticity in the intrinsic excitability of neurons is based on dynamic changes in the expression, localization, and/or functional properties of voltage-gated ion channels. Kv channels are the most diverse family of voltage-gated channels and as such are primary determinants of diversity of overall neuronal excit-

ability and of the input-output relationships in mammalian neurons (34). A number of recent studies have provided valuable insights into the role of specific Kv channel subtypes in the processing and integration of synaptic input within the somatodendritic domain (35), initiation and propagation of axonal action potentials (36), and regulation of neurotransmitter release (37). Modulation of the abundance, subcellular distribution, and gating of Kv channels through reversible multisite phosphorylation has emerged as a common theme for dynamic regulation of neuronal function (34, 38, 39) by allowing for integration between cell signaling pathways impacting the activity of specific neuronal PKs and PPs and the ion channels crucial for regulating neuronal excitability. Prominent examples include enhanced excitatory synaptic activity causing PKA-dependent phosphorylation and internalization of Kv4.2 in dendritic spines that results in enhancement of mEPSCs in hippocampal neurons (40, 41) and high frequency auditory stimulation causing rapid dephosphorylation of Kv3.1, leading to the enhancement of Kv3.1 activity needed to support high frequency spiking in auditory neurons (42). As detailed above, Kv2.1 is subjected to extensive bidirectional activity-dependent changes in phosphorylation state, changing its localization and function to homeostatically regulate neuronal excitability.

Here we show that CDK5 is the key PK for determining the Kv2.1 phosphorylation state in neurons, including at the Ser-603 site that is key to phosphorylation-dependent regulation of Kv2.1 gating (15) and at other sites that regulate Kv2.1 clustering. CDK5 can directly phosphorylate the recombinant Kv2.1 C terminus as well as Kv2.1 purified from mammalian brain. Moreover, we show here that CDK5 is responsible for Kv2.1 phosphorylation under diverse conditions of neuronal activity, including determining the constitutive level of Kv2.1 phosphorylation, the enhanced Kv2.1 phosphorylation that occurs after acute activity blockade, and the recovery of Kv2.1 phosphorylation after activity-dependent dephosphorylation. As such, CDK5 is poised to be a key determinant of the activity-dependent changes in Kv2.1 expression, localization, and function that have been found to underlie certain forms of plasticity in intrinsic excitability. Previous studies have established a clear role for CDK5 activity in nervous system development, such that inhibition, ablation, or knockdown of CDK5 leads to defects in neuronal migration, maturation, and survival (43). CDK5 has also been implicated as a key player in synaptic plasticity, with actions on both postsynaptic neurotransmitter receptors and presynaptic neurotransmitter release (19). Although CDK5 has been recently implicated in regulating constitutive biosynthetic trafficking of neuronal Kv1 channels to the axon initial segment (44), a role for CDK5 in dynamic, reversible modulation of Kv channels or of other neuronal ion channels has not been described previously.

We show here that CDK5 activity is required for the recovery of the phosphorylation and clustering of Kv2.1 protein after an episode of activity-induced, calcineurin-dependent dephosphorylation. Excitatory stimulation (*e.g.* glutamatergic stimulation or depolarization) has been found to reduce CDK5 activity in neurons, due to degradation of p35 and p39 regulatory subunits (28, 30). Subsequent recovery of the expression level of these subunits and therefore of CDK5 activity begins at 90 min after washout of the stimulus (31), similar to the kinetics shown here and elsewhere (5, 9) for recovery of Kv2.1 phosphorylation. As such, our findings are consistent with a mechanism whereby *de novo* synthesis of obligatory p35/p39 subunits and their association in active CDK5 complexes is the rate-limiting step in the recovery of Kv2.1 phosphorylation after calcineurin-dependent dephosphorylation in response to excitatory stimulation. Whether changes in the activity of neuronal PPs (PP1 and/or calcineurin) or PKs other than CDK5 are also involved in determining other aspects of the recovery of Kv2.1 phosphorylation is at yet unknown. It is intriguing, given their opposing roles in regulating Kv2.1, that CDK5 and calcineurin also have counteracting activity-dependent effects on synaptic vesicle endocytosis, via phosphorylation of components of the release machinery (45, 46).

We found that the CDK inhibitor roscovitine blocks the increased phosphorylation of Kv2.1 induced by acute neuronal activity blockade. That Kv2.1 is a direct substrate for CDK5 *in vitro* suggests that the enhanced Kv2.1 phosphorylation upon activity blockade is due to increased CDK5 activity and direct CDK5 phosphorylation of Kv2.1. Whereas the activity of most other PKs is under the control of either second messengers (*e.g.* cAMP, Ca^{2+}, DAG, etc.) or phosphorylation cascades involving other PKs or PPs, either of which can be rapidly modulated by neuronal signaling pathways, all available evidence suggests that CDK5 activity is exclusively regulated by the levels of its obligatory p35 and p39 subunits, as determined by their *de novo* synthesis and degradation (47). Rapid activity-dependent down-regulation of CDK5 activity is achieved by triggered degradation of p35/p39 in response to neuronal depolarization (28, 45) and NMDA stimulation (30). Acute up-regulation of CDK5 activity would therefore require rapid *de novo* synthesis of p35 and/or p39 and their association with plasma membrane-localized CDK5, events unlikely to occur within the short time frame of acute activity blockade (15 min) that we found induces enhanced Kv2.1 phosphorylation. Extensive relocalization of CDK5 in response to excitotoxic stimulation occurs through calpain-mediated cleavage of the myristoylated region from p35, leading to loss of the plasma membrane association of the CDK5 complex and its translocation into the cytoplasm and resulting in phosphorylation of non-physiological CDK5 substrates and neurotoxicity nucleus (48). Although changes in the subcellular localization of the obligatory subunits or of preexisting active CDK5 complexes to sites of high density Kv2.1 clustering could underlie the rapid increase in Kv2.1 phosphorylation upon acute activity blockade, relocalization of CDK5 and its regulatory subunits to access different plasma membrane substrates has not been described. Interestingly, a previous study revealed a slight increase in DARPP-32 phosphorylation at Thr-75, a known CDK5 phosphorylation site, in response to short (10-min) TTX treatment (49), providing additional suggestive evidence for rapid activation of CDK5 in response to acute activity blockade. Future studies will determine the mechanisms whereby CDK5 activity can be rapidly stimulated by acute activity blockade and how it then acts via phosphorylation of Kv2.1 and other substrates to mediate responses to decreased neuronal activity.

We found that pharmacological inhibition of PP1 in unstimulated neurons dramatically increases phosphorylation of Kv2.1 at the CDK5-dependent Ser-603 phosphorylation site. This is in sharp contrast to calcineurin inhibitors, which have little effect on constitutive phosphorylation of Kv2.1 but abolish the rapid dephosphorylation of Kv2.1 in response to excitatory stimuli (5, 7). We found that PP1 overexpression leads to decreased Kv2.1 phosphorylation in heterologous cells and that PP1, like calcineurin (7), can directly dephosphorylate immunopurified Kv2.1 *in vitro*. PP1 is involved in diverse aspects of neuronal plasticity (50), and ion channels are prominent targets for PP1-mediated dephosphorylation (51). Interestingly, PP1 activity is negatively regulated by CDK5 phosphorylation, via inhibitory phosphorylation at the Thr-320 site on PP1 (32, 33). As such, inhibition of CDK5 could lead to enhanced PP1 activity, driving the dephosphorylation of Kv2.1 via an indirect mechanism that is not dependent on reduced CDK5-mediated Kv2.1 phosphorylation. We showed here that the effects of expressing a mutant PP1 (PP1-T320A) that is resistant to CDK5-mediated inhibition were indistinguishable from those of WT PP1, supporting a role for direct CDK5-mediated phosphorylation of Kv2.1 as the primary determinant of the rapid increase in Kv2.1 phosphorylation seen upon acute activity blockade and during the recovery period following excitation-induced, calcineurin-mediated, Kv2.1 dephosphorylation. However, because PP1 activity does seem to be important in establishing the steady-state level of Kv2.1 phosphorylation, its possible contributions to regulating Kv2.1 phosphorylation during these other processes cannot be completely discounted. Future studies will reveal the precise interplay between CDK5 and neuronal PPs, such as PP1 and calcineurin, in determining the phosphorylation state of Kv2.1 and of other ion channels whose modulation alters intrinsic excitability and that act as the molecular substrates for intrinsic neuronal plasticity.

Acknowledgments—We thank Dr. Li-Huei Tsai (MIT) for providing the pcDNA-GFP-CDK5-D144N, pcDNA3-GFP-CDK5, and pCMV-myc-p35 plasmids (via Addgene, plasmids 1344, 1346, and 1347, respectively) and Dr. Hemant Paudel (McGill University) for providing the pcDNA-myc-PP1 and pcDNA-myc-PP1 (T320A). Mass spectrometry was performed at the University of California Davis Proteomics Facility. We are grateful to Ashleigh Evans for critical comments on the manuscript and to Jesus Aguado, Ada Kan, Linda Sah, and Rachel Silverman for technical assistance.

REFERENCES

1. Baranauskas, G., Tkatch, T., and Surmeier, D. J. (1999) *J. Neurosci.* **19,** 6394–6404
2. Murakoshi, H., and Trimmer, J. S. (1999) *J. Neurosci.* **19,** 1728–1735
3. Guan, D., Tkatch, T., Surmeier, D. J., Armstrong, W. E., and Foehring, R. C. (2007) *J. Physiol.* **581,** 941–960
4. Murakoshi, H., Shi, G., Scannevin, R. H., and Trimmer, J. S. (1997) *Mol. Pharmacol.* **52,** 821–828
5. Misonou, H., Mohapatra, D. P., Park, E. W., Leung, V., Zhen, D., Misonou, K., Anderson, A. E., and Trimmer, J. S. (2004) *Nat. Neurosci.* **7,** 711–718
6. Misonou, H., Mohapatra, D. P., Menegola, M., and Trimmer, J. S. (2005) *J. Neurosci.* **25,** 11184–11193
7. Misonou, H., Menegola, M., Mohapatra, D. P., Guy, L. K., Park, K. S., and Trimmer, J. S. (2006) *J. Neurosci.* **26,** 13505–13514
8. Misonou, H., Thompson, S. M., and Cai, X. (2008) *J. Neurosci.* **28,** 8529–8538
9. Mulholland, P. J., Carpenter-Hyland, E. P., Hearing, M. C., Becker, H. C., Woodward, J. J., and Chandler, L. J. (2008) *J. Neurosci.* **28,** 8801–8809
10. Aras, M. A., Saadi, R. A., and Aizenman, E. (2009) *Eur. J. Neurosci.* **30,** 2250–2257
11. Mulholland, P. J., Carpenter-Hyland, E. P., Woodward, J. J., and Chandler, L. J. (2009) *Alcohol* **43,** 45–50
12. Ito, T., Nuriya, M., and Yasui, M. (2010) *Neurobiol. Dis.* **38,** 85–91
13. Mohapatra, D. P., Misonou, H., Pan, S. J., Held, J. E., Surmeier, D. J., and Trimmer, J. S. (2009) *Channels* **3,** 46–56
14. Nataraj, K., Le Roux, N., Nahmani, M., Lefort, S., and Turrigiano, G. (2010) *Neuron* **68,** 750–762
15. Park, K. S., Mohapatra, D. P., Misonou, H., and Trimmer, J. S. (2006) *Science* **313,** 976–979
16. Park, K. S., Mohapatra, D. P., and Trimmer, J. S. (2007) *Channels* **1,** 59–61
17. Tsai, L. H., Delalle, I., Caviness, V. S., Jr., Chae, T., and Harlow, E. (1994) *Nature* **371,** 419–423
18. Cai, X. H., Tomizawa, K., Tang, D., Lu, Y. F., Moriwaki, A., Tokuda, M., Nagahata, S., Hatase, O., and Matsui, H. (1997) *Neurosci. Res.* **28,** 355–360
19. Lai, K. O., and Ip, N. Y. (2009) *Biochim. Biophys. Acta* **1792,** 741–745
20. Shi, G., Kleinklaus, A. K., Marrion, N. V., and Trimmer, J. S. (1994) *J. Biol. Chem.* **269,** 23204–23211
21. Trimmer, J. S. (1991) *Proc. Natl. Acad. Sci. U.S.A.* **88,** 10764–10768
22. Chen, Y., Stevens, B., Chang, J., Milbrandt, J., Barres, B. A., and Hell, J. W. (2008) *J. Neurosci. Methods* **171,** 239–247
23. Lim, S. T., Antonucci, D. E., Scannevin, R. H., and Trimmer, J. S. (2000) *Neuron* **25,** 385–397
24. Berendt, F. J., Park, K. S., and Trimmer, J. S. (2010) *J. Proteome Res.* **9,** 1976–1984
25. Racine, R. J. (1972) *Electroencephalogr. Clin. Neurophysiol.* **32,** 281–294
26. Trinidad, J. C., Thalhammer, A., Specht, C. G., Lynn, A. J., Baker, P. R., Schoepfer, R., and Burlingame, A. L. (2008) *Mol. Cell Proteomics* **7,** 684–696
27. Wiśniewski, J. R., Nagaraj, N., Zougman, A., Gnad, F., and Mann, M. (2010) *J. Proteome Res.* **9,** 3280–3289
28. Schuman, E. M., and Murase, S. (2003) *Philos. Trans. R. Soc. Lond. B Biol. Sci.* **358,** 749–756
29. Buraei, Z., Schofield, G., and Elmslie, K. S. (2007) *Neuropharmacology* **52,** 883–894
30. Wei, F. Y., Tomizawa, K., Ohshima, T., Asada, A., Saito, T., Nguyen, C., Bibb, J. A., Ishiguro, K., Kulkarni, A. B., Pant, H. C., Mikoshiba, K., Matsui, H., and Hisanaga, S. (2005) *J. Neurochem.* **93,** 502–512
31. Hosokawa, T., Saito, T., Asada, A., Ohshima, T., Itakura, M., Takahashi, M., Fukunaga, K., and Hisanaga, S. (2006) *J. Neurosci. Res.* **84,** 747–754
32. Dohadwala, M., da Cruz e Silva, E. F., Hall, F. L., Williams, R. T., Carbonaro-Hall, D. A., Nairn, A. C., Greengard, P., and Berndt, N. (1994) *Proc. Natl. Acad. Sci. U.S.A.* **91,** 6408–6412
33. Li, T., Chalifour, L. E., and Paudel, H. K. (2007) *J. Biol. Chem.* **282,** 6619–6628
34. Johnston, J., Forsythe, I. D., and Kopp-Scheinpflug, C. (2010) *J. Physiol.* **588,** 3187–3200
35. Johnston, D., Christie, B. R., Frick, A., Gray, R., Hoffman, D. A., Schexnayder, L. K., Watanabe, S., and Yuan, L. L. (2003) *Philos. Trans. R. Soc. Lond. B Biol. Sci.* **358,** 667–674
36. Kress, G. J., and Mennerick, S. (2009) *Neuroscience* **158,** 211–222
37. Dodson, P. D., and Forsythe, I. D. (2004) *Trends Neurosci.* **27,** 210–217
38. Cerda, O., and Trimmer, J. S. (2010) *Neurosci. Lett.* **486,** 60–67
39. Shah, M. M., Hammond, R. S., and Hoffman, D. A. (2010) *Trends Neurosci.* **33,** 307–316
40. Kim, J., Jung, S. C., Clemens, A. M., Petralia, R. S., and Hoffman, D. A. (2007) *Neuron* **54,** 933–947
41. Hammond, R. S., Lin, L., Sidorov, M. S., Wikenheiser, A. M., and Hoffman, D. A. (2008) *J. Neurosci.* **28,** 7513–7519
42. Song, P., Yang, Y., Barnes-Davies, M., Bhattacharjee, A., Hamann, M., Forsythe, I. D., Oliver, D. L., and Kaczmarek, L. K. (2005) *Nat. Neurosci.* **8,** 1335–1342
43. Jessberger, S., Gage, F. H., Eisch, A. J., and Lagace, D. C. (2009) *Trends Neurosci.* **32,** 575–582

44. Vacher, H., Yang, J. W., Cerda, O., Autillo-Touati, A., Dargent, B., and Trimmer, J. S. (2011) *J. Cell Biol.* **192,** 813–824
45. Tan, T. C., Valova, V. A., Malladi, C. S., Graham, M. E., Berven, L. A., Jupp, O. J., Hansra, G., McClure, S. J., Sarcevic, B., Boadle, R. A., Larsen, M. R., Cousin, M. A., and Robinson, P. J. (2003) *Nat. Cell Biol.* **5,** 701–710
46. Tomizawa, K., Sunada, S., Lu, Y. F., Oda, Y., Kinuta, M., Ohshima, T., Saito, T., Wei, F. Y., Matsushita, M., Li, S. T., Tsutsui, K., Hisanaga, S., Mikoshiba, K., Takei, K., and Matsui, H. (2003) *J. Cell Biol.* **163,** 813–824
47. Hisanaga, S., and Saito, T. (2003) *Neurosignals* **12,** 221–229
48. Lee, M. S., Kwon, Y. T., Li, M., Peng, J., Friedlander, R. M., and Tsai, L. H. (2000) *Nature* **405,** 360–364
49. Nishi, A., Bibb, J. A., Matsuyama, S., Hamada, M., Higashi, H., Nairn, A. C., and Greengard, P. (2002) *J. Neurochem.* **81,** 832–841
50. Munton, R. P., Vizi, S., and Mansuy, I. M. (2004) *FEBS Lett.* **567,** 121–128
51. Dai, S., Hall, D. D., and Hell, J. W. (2009) *Physiol. Rev.* **89,** 411–452